

Supporting Information

Interconversion of the Pallambins through Photo-induced Rearrangement

Jiao-Zhen Zhang,^{†,§} Rong-Xiu Zhu,^{‡,§} Gang Li,^{†,§} Li-Ning Wang,[†] Bin Sun,[†] Wen-Fang Chen,[†]
Lei Liu,[†] and Hong-Xiang Lou^{*,†}

[†] *Department of Natural Products Chemistry, Key Lab of Chemical Biology (MOE), School of Pharmaceutical Sciences, Shandong University, No. 44 West Wenhua Road, Jinan 250012, People's Republic of China. Fax: (+86) 531-8838-2019; Tel: (+86) 531-8838-2012; E-mail: louhongxiang@sdu.edu.cn*

[‡] *School of Chemistry and Chemical Engineering, Shandong University, No. 27 Shanda Nanlu, Jinan 250100, People's Republic of China.*

[§] *Jiao-Zhen Zhang, Rong-Xiu Zhu, and Gang Li contributed equally to this work.*

List of supporting information

Experimental Section

1. General experimental procedures
2. HPLC analysis
3. UV analysis
4. Laser flash photolysis (LFP) experiment
5. Theory and calculation details

Figures S1–S17

Table S1

References for Supporting Information.

Experimental Section

1. General experimental procedures. UV data were recorded on a UV-2450 spectrophotometer (Shimadzu, Japan). Fluorescence spectrum was measured with an F-7000 FL spectrophotometer. The transient absorption spectra were obtained on a nanosecond laser flash photolysis apparatus, in which the 266 nm excitation was generated by the Quanta Ray GCR-150 Nd: YAG laser (Spectra-Physics, laser energy 10 mJ/pulse, pulse width 5-6 ns, repetition rate 10 Hz). The transients were monitored with a xenon arclamp (OSRAM, XBO 150 W/CR-OFR), and the signals from the differential amplifier (R928 photomultiplier, 5-stage) were collected by a digitizing oscilloscope (Agilent 54820A, 2 GSa/s) connected to the work station (Acorn). HPLC were performed on an Agilent Technologies 1260 infinity equipped with an Agilent Eclipse XDB-C₁₈ 5 μ m column (4.6 \times 250 mm). All solvents used were of analytical grade.

2. HPLC analysis. 0.5 mg **3** or **4** was added to test tube to perform the photoinduced reaction. Compound **3** or **4** was dissolved in 1 ml of anhydrous acetonitrile and the dissolved oxygen in the solution was removed by bubbling with nitrogen for 30 min. The solution was irradiated (RPR-2537A Lamps, 400 W) at 35 °C under a nitrogen atmosphere. The light intensity was about 2 mW/cm². Analytical HPLC was used to analyze the changes of compounds. The flow rate was 1.0 ml/min and the elution was accomplished with water and acetonitrile (1:1 by volume). Samples (4 μ l) were injected directly at various time points (0, 3, 6, 15, 30, 60, 120, 130 min). Moreover, the composition of liverwort *Pallavicinia ambigua* was also analyzed to determine the presence of compounds **1–4** in nature. Pure pallambins A–D (**1–4**) we isolated from this liverwort were used to compare their retention times with those of compounds in reaction solution and plant (Figure S1 and S2).

By applying the same strategy as above, the photochemical reaction for compound **3** (12.4 mg) was subjected to semi-preparative HPLC in the reversed phase mode to afford **1** (3.25 mg, 26% yield) and **2** (3.70 mg, 30% yield). The ¹H NMR spectra of these compounds are shown in figures S13 and S14.

3. UV analysis. 0.035 mg compound **3** or **4** was dissolved in 4 ml of anhydrous acetonitrile. The solution in a quartz cell (1 cm optical pathlength) was deoxygenated by nitrogen bubbling for 20 min prior to irradiation. Then the cell was closed using a septum. The solution was irradiated (RPR-2537A Lamps, 400 W) at 35 °C and the light intensity was about 2 mW/cm². UV absorption spectroscopy was measured at various time points.

4. Laser flash photolysis (LFP) experiment. The transient absorption spectra were recorded after 266-nm laser flash photolysis of the solution of samples. The solution of 0.5 mmol/L compound **3** for LFP experiment was prepared with spectroscopic grade CH₃CN, and was then deaerated or aerated by nitrogen or oxygen bubbling for 30 min. The decay data from this photolysis technique were obtained by measuring

the kinetics at specific wavelengths at 10 nm intervals between 250 nm and 380 nm. The decay trends of transient absorbance at specific wavelengths from 250 to 380 nm showed that within the 50 ns, the luminescence (fluorescence) appeared but had different lifetimes (Figure S5 and S6), which suggested that there may be transient absorption of the intermediates involved in this period. According to the proportion of absorbance at specific wavelengths in fluorescence spectrum (Figure S4), we assigned the decay absorption of 280 nm as basic curve, and then deduct proportionally the basic decay absorption to get the time-resolved transient absorption spectra of transient species.

Laser flash photolysis (LFP) studies with 266 nm excitation of a solution of compound **3** in acetonitrile gave the time-resolved transient absorption spectra at the range from 290 to 360 nm (Figure S7). The presence of a transient species was confirmed by the evidence that the absorption spectra grew within 16.2 ns after laser pulse before decayed proportionally. And it decayed on a time scale of merely tens of nanoseconds. The triplet excited state of this intermediate was also involved in this photochemical reaction as suggested by the significant influence of oxygen on transient absorption (Figure S8). Thus, in the photolysis of nitrogen-saturated acetonitrile solution of **3**, only one reactive intermediate was detected in this photoreaction, which may imply that the lifetime of this transient is longer.

5. Theory and calculation details. Our calculations were carried out with the Gaussian 09 software package¹ under the framework of density functional theory (DFT) with UB3LYP functional.² The standard 6-31G (d) basis set was used for all atoms. Broken spin symmetry UBS methods at the same level was employed for the singlet species. Geometries of minima and transition states were completely optimized by total energy minimization with the use of analytic gradient techniques. Harmonic vibrational frequency calculations have also been conducted to verify all stationary points as minima (zero imaginary frequency) or first-order saddle points (one imaginary frequency). To obtain more reliable energies, single point energy calculations of all species involved in this work were further carried out by using the more flexible basis set 6-311++G(2d, p). For all cited energies, thermal corrections to Gibbs free energy have been included.

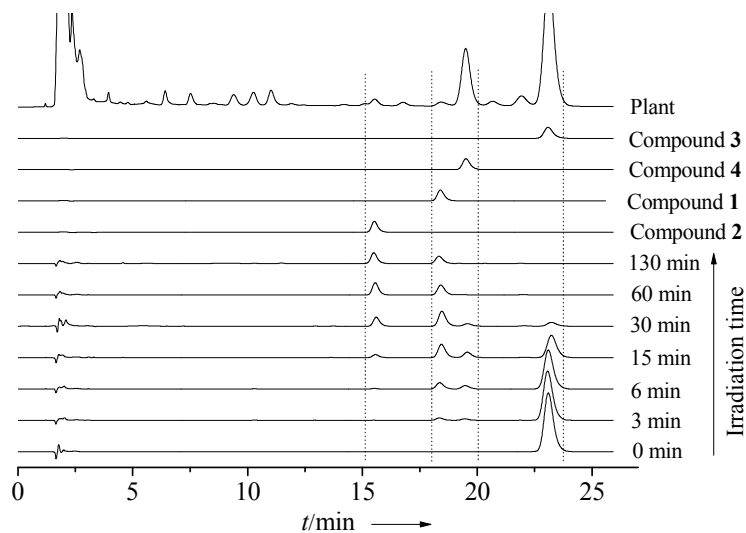


Figure S1. HPLC chromatograms ($\lambda_{\text{detection}} = 210 \text{ nm}$) as a function of irradiation time obtained for the irradiation of compound **3** in nitrogen-saturated acetonitrile solution ($\lambda_{\text{excitation}} = 254 \text{ nm}$), and HPLC analysis of the liverwort *Pallavicinia ambigua*.

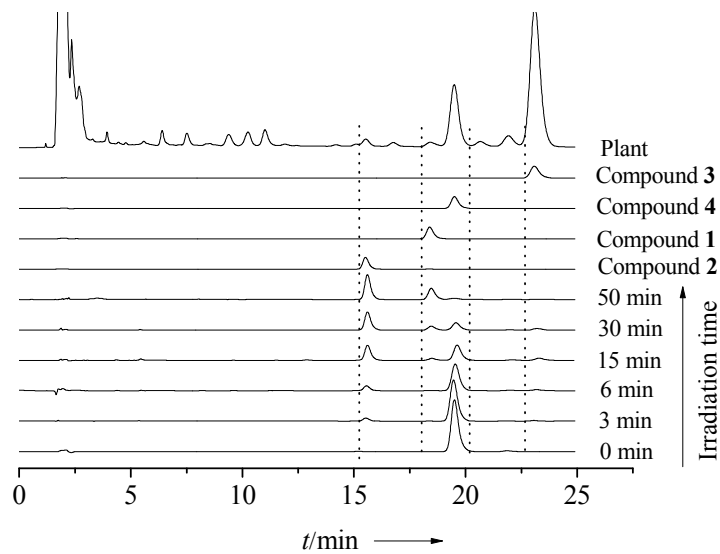


Figure S2. HPLC chromatograms ($\lambda_{\text{detection}} = 210 \text{ nm}$) as a function of irradiation time obtained for the irradiation of compound **4** in nitrogen-saturated acetonitrile solution ($\lambda_{\text{excitation}} = 254 \text{ nm}$), and HPLC analysis of the liverwort *Pallavicinia ambigua*.

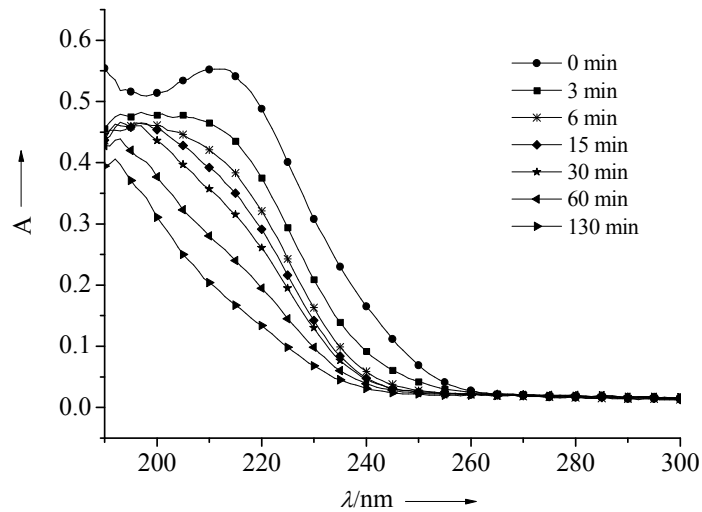


Figure S3. Changes in the UV absorption spectra of nitrogen-saturated acetonitrile solution for compound **4** irradiated by 254 nm light.

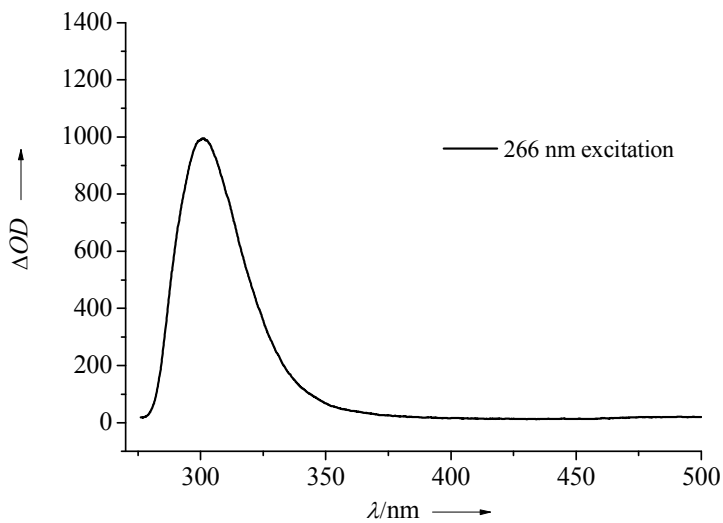


Figure S4. The fluorescence emission spectra of compound **3** ($\lambda_{\text{excitation}} = 266 \text{ nm}$).

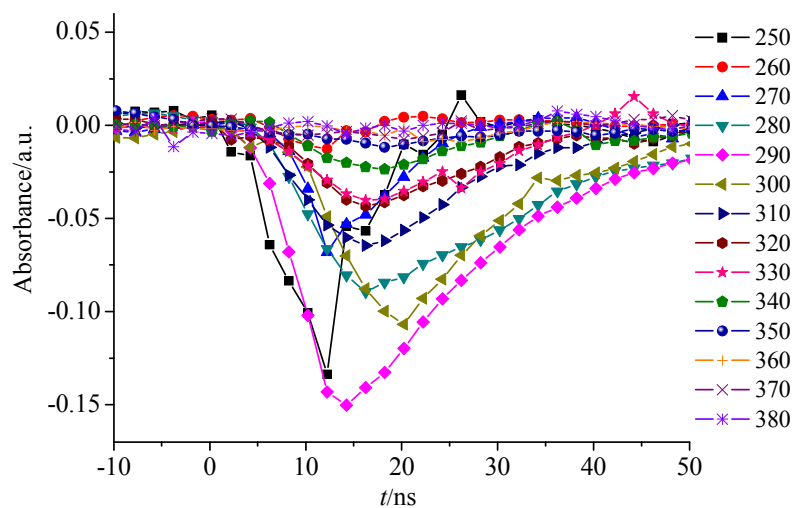


Figure S5. Kinetic trends of transient absorbance in the photolysis of N_2 -saturated CH_3CN solution of **3** at specific wavelengths between 250 nm and 380 nm.

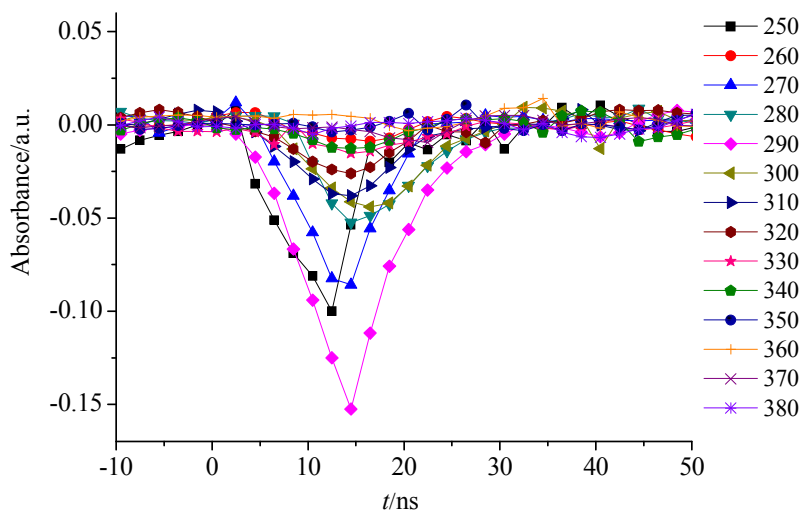


Figure S6. Kinetic trends of transient absorbance in the photolysis of O_2 -saturated CH_3CN solution of **3** at specific wavelengths between 250 nm and 380 nm.

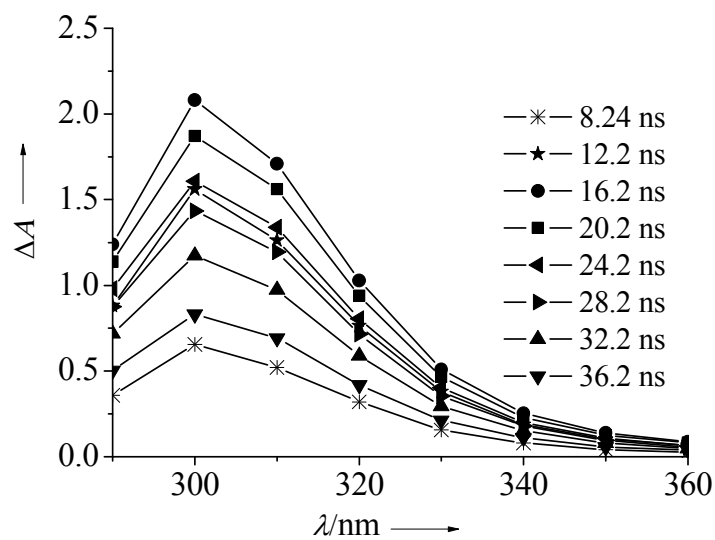


Figure S7. Transient absorption spectra for N₂-saturated CH₃CN solution of **3**.

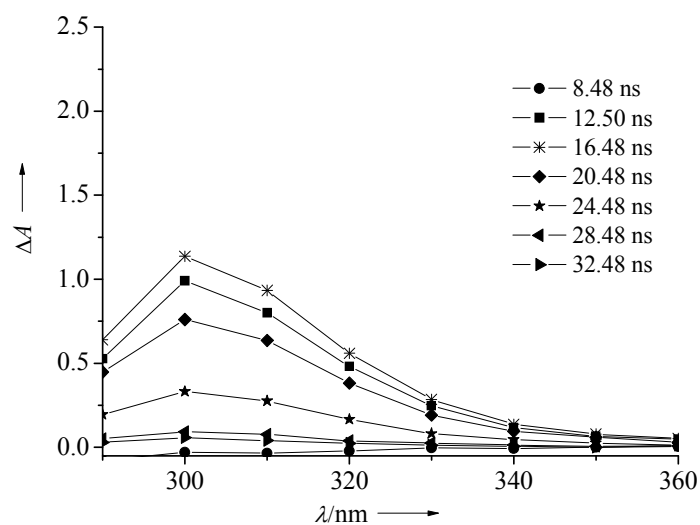


Figure S8. Transient absorption spectra for O₂-saturated CH₃CN solution of **3**.

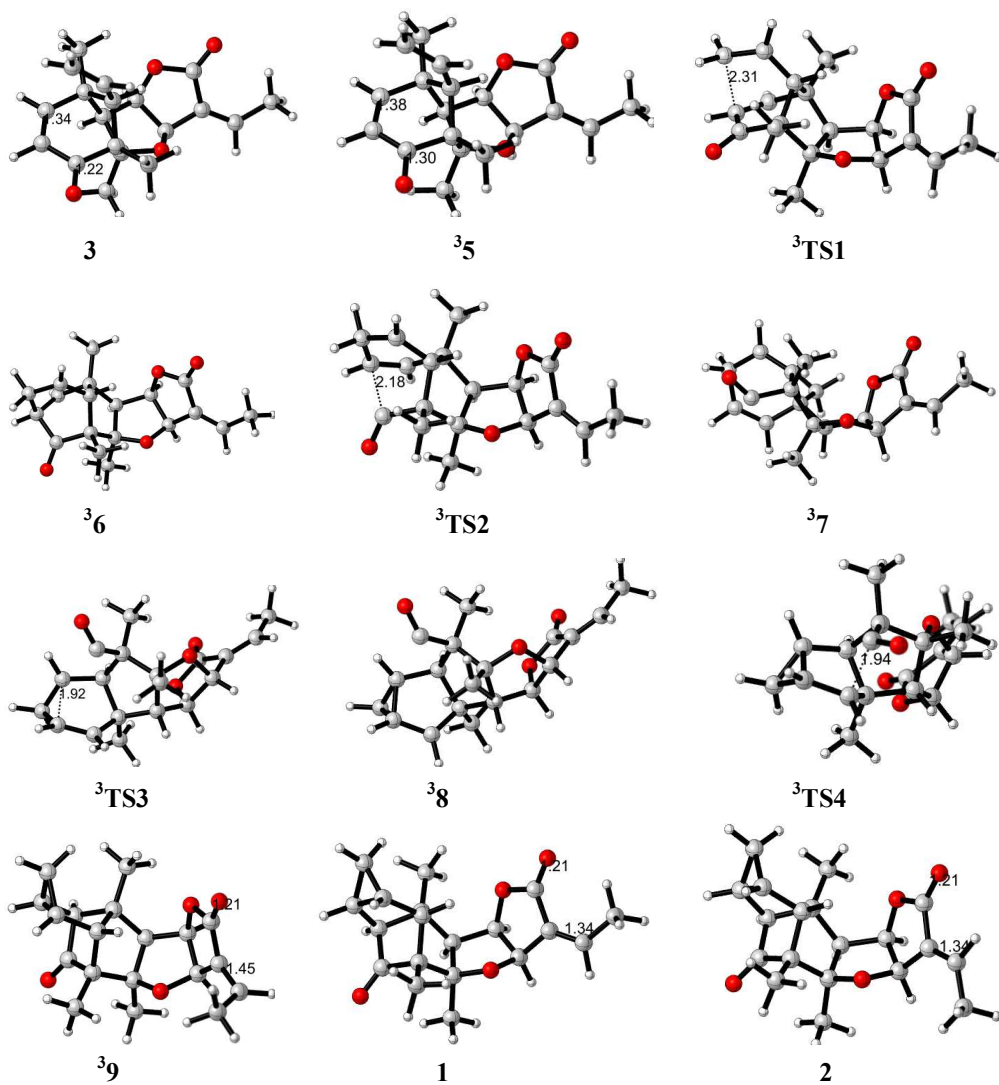


Figure S9. Optimized geometry of intermediates and transition states with main geometrical parameters along the reaction coordinates for the triplet biradical reaction pathway of **3** to produce the compounds **1** and **2**.

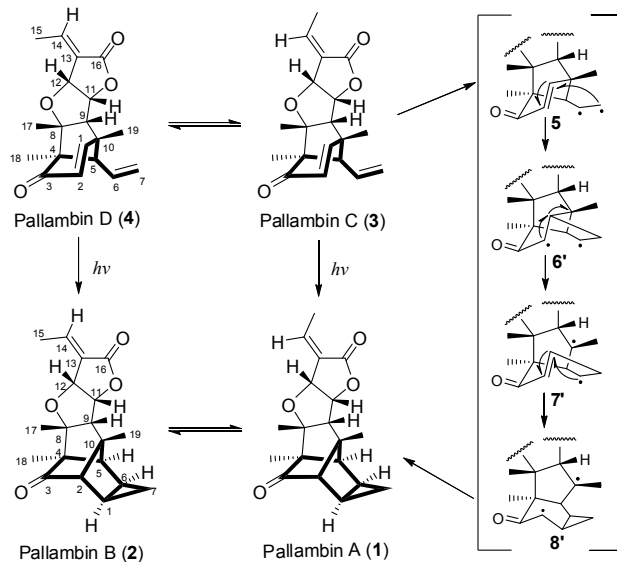


Figure S10. Proposed an alternative mechanism for the formation of **1** and **2** through sequential radical addition and cyclization.

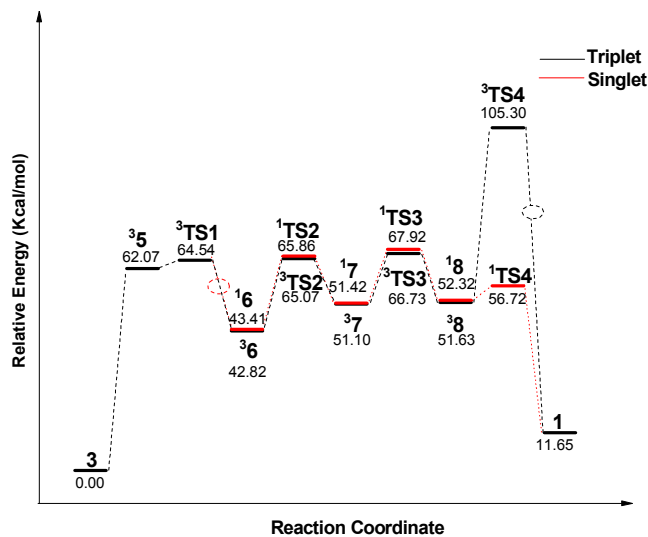


Figure S11. The potential energy profiles for the photochemical reaction of **3** to produce the compound **1** along an alternative pathway, where the circles mean intercrossing-system between the triplet–singlet surfaces.

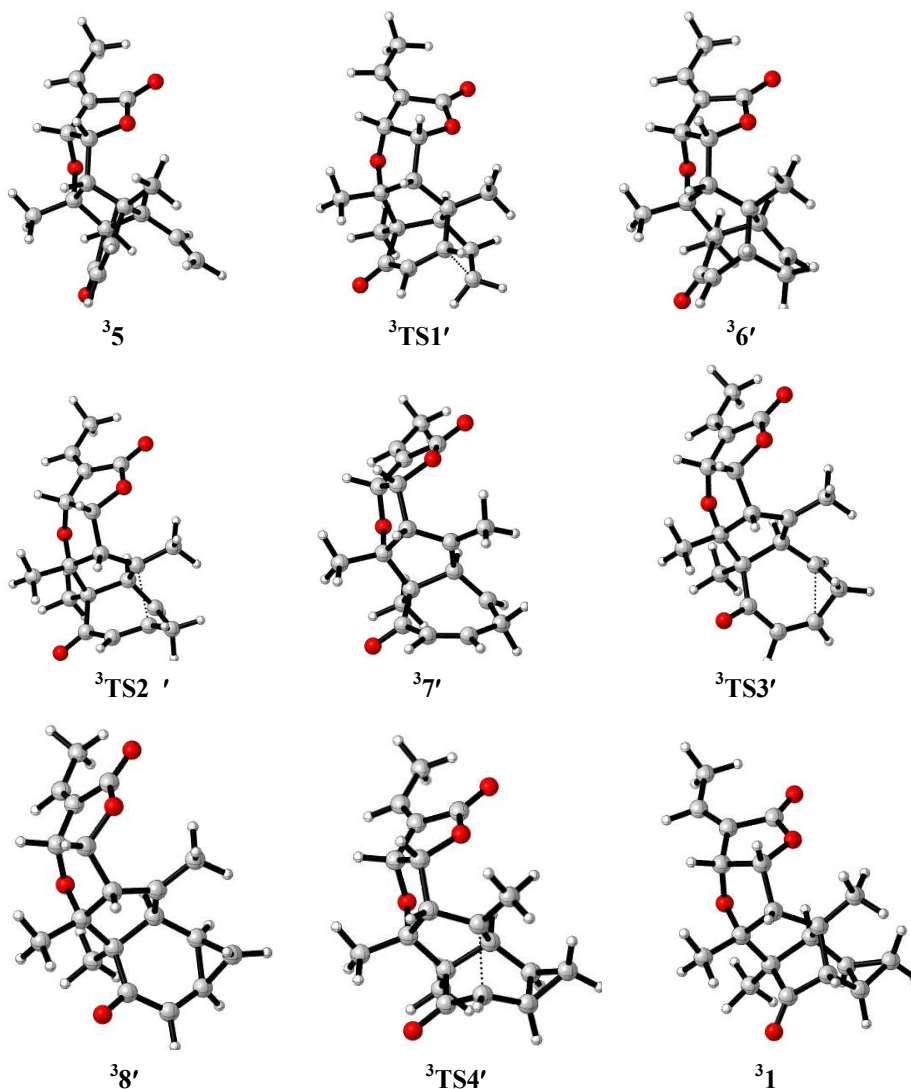


Figure S12. The transition states (TSs) involved in the mechanism of light-induced radical reaction along an alternative pathway.

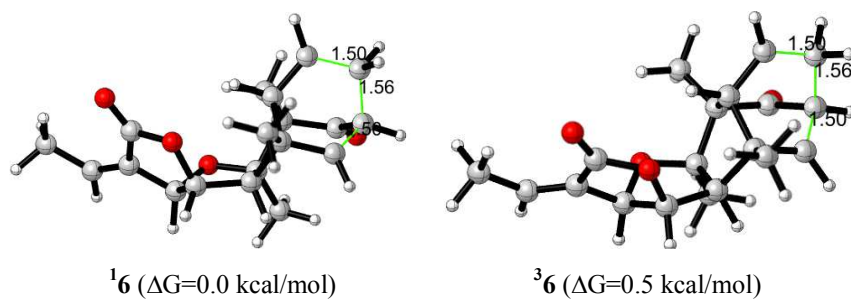


Figure S13. DFT optimized geometries of the triplet and singlet 1,4-diradical species with key geometrical parameters. The relative free energies are given in parentheses

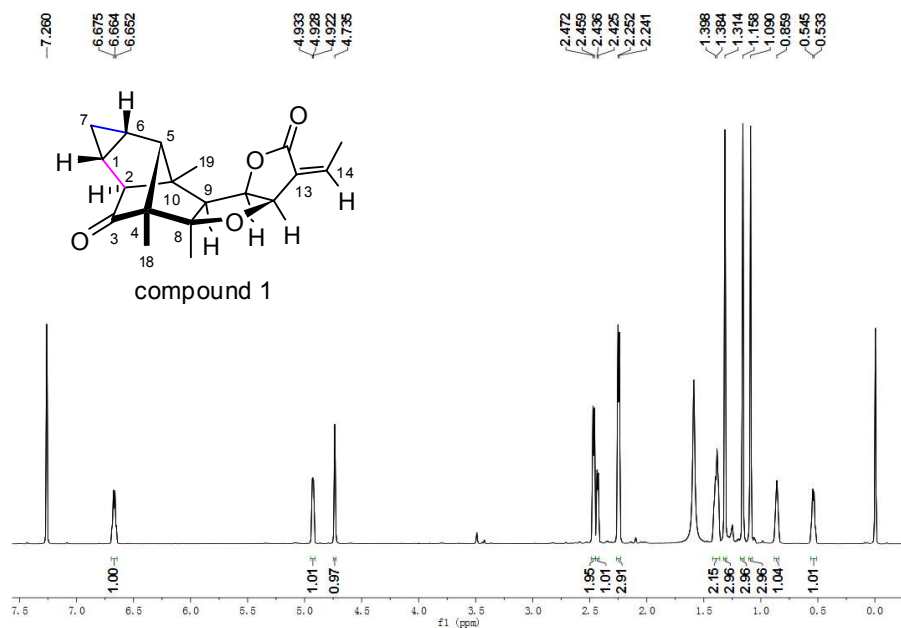


Figure S14. ^1H NMR spectrum (600 MHz) of **1** in CDCl_3 (Compound **1** was obtained from the photochemical reaction by HPLC).

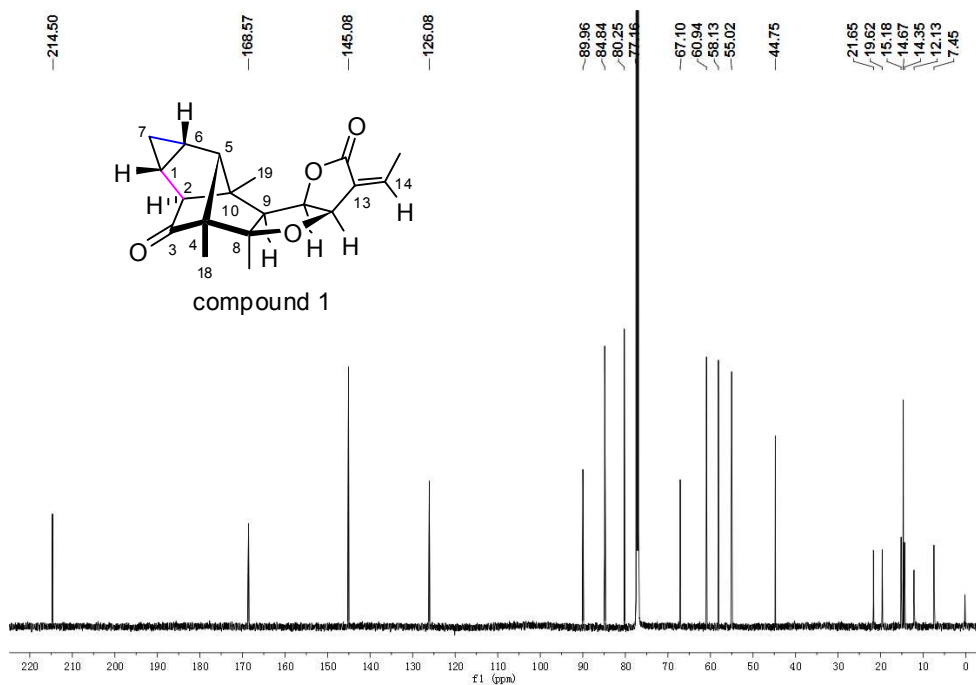


Figure S15. ^{13}C NMR spectrum (150 MHz) of **1** in CDCl_3 (Compound **1** was obtained from the photochemical reaction by HPLC).

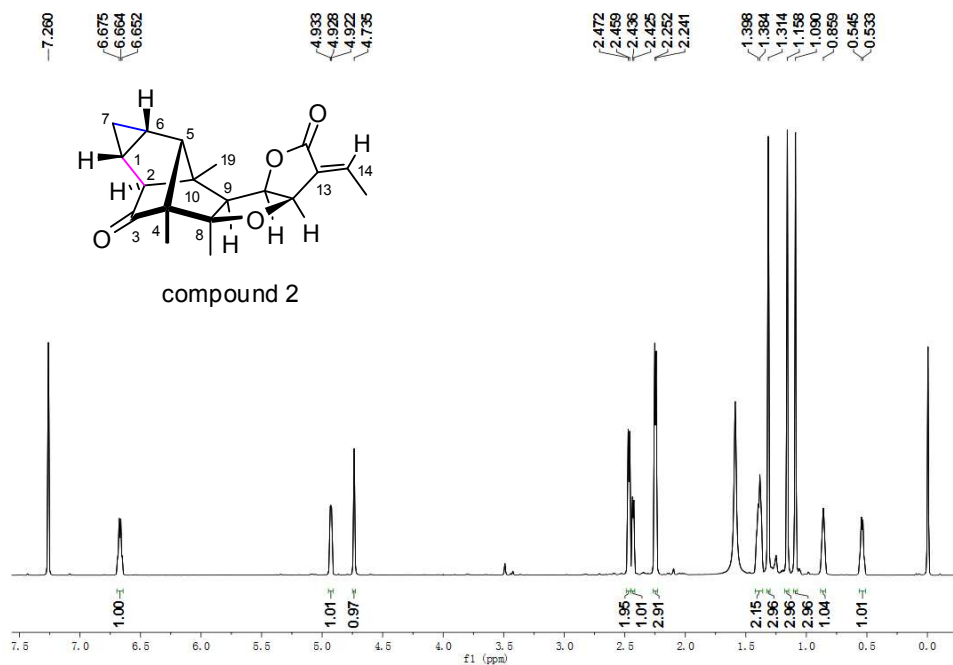


Figure S16. ^1H NMR spectrum (600 MHz) of **2** in CDCl_3 (Compound **2** was obtained from the photochemical reaction by HPLC).

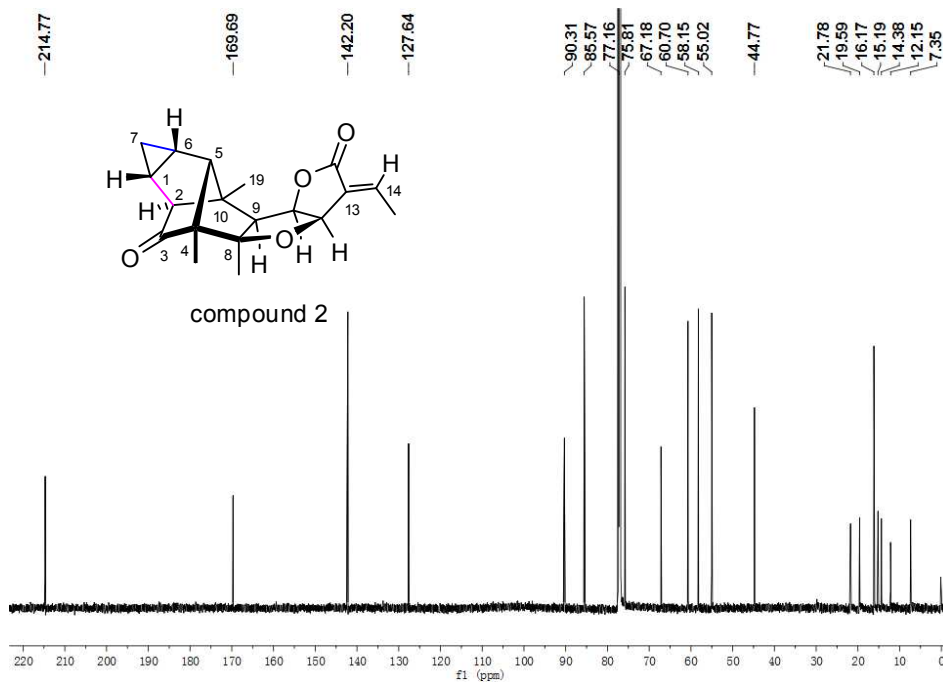


Figure S17. ^{13}C NMR spectrum (150 MHz) of **2** in CDCl_3 (Compound **2** was obtained from the photochemical reaction by HPLC).

Table S1. ^1H and ^{13}C NMR data of **1** and **2** (in CDCl_3)^a

position	1		2	
	δ_{H} (mult, J)	δ_{C}	δ_{H} (mult, J)	δ_{C}
1	1.40 (m)	14.7	1.38 (m)	14.4
2	2.47 (br s)	58.1	2.48 (br s)	58.2
3		214.5		214.8
4		67.1		67.2
5	2.46 (br s)	55.0	2.40 (br s)	55.0
6	0.86 (br s)	15.2	0.86 (br s)	15.2
7 α	0.54 (q, 7.2)	12.1	0.54 (q, 6.6)	12.2
7 β	1.38 (m)		1.37 (m)	
8		90.0		90.3
9	2.43 (d, 6.6)	60.9	2.46 (d, 6.6)	60.7
10		44.8		44.8
11	4.93 (m)	84.8	4.96 (m)	85.6
12	4.76 (br s)	80.3	4.97 (m)	75.8
13		126.1		127.6
14	6.67 (q, 7.2)	145.1	7.01 (q, 7.2)	142.2
15	2.25 (3H, d, 6.6)	14.4	2.02 (3H, d, 6.6)	16.2
16		168.6		169.7
17	1.09 (3H, s)	19.8	1.11 (3H, s)	19.6
18	1.16 (3H, s)	7.5	1.14 (3H, s)	7.4
19	1.31 (3H, s)	21.9	1.32 (3H, s)	21.8

^a Recorded at 600 MHz (^1H NMR) or 150 MHz (^{13}C NMR). J in Hz.

References for Supporting Information.

- (1) Frisch, M. J.; Trucks, G. W.; Schlegel, H. B.; Scuseria, G. E.; Robb, M. A.; Cheeseman, J. R. et al. *Gaussian 09*, revision A.1; Gaussian, Inc.: Wallingford, CT, 2009.
- (2) (a) Becke, A. D. *J. Chem. Phys.* **1993**, *98*, 1372–1377. (b) Becke, A. D. *J. Chem. Phys.* **1993**, *98*, 5648–5652. (c) Becke, A. D. *Phys. Rev. A* **1988**, *38*, 3098–3100.
- (d) Lee, C.; Yang, W.; Parr, R. G. *Phys. Rev. B* **1988**, *37*, 785–789.